Record-low Arctic stratospheric ozone in 2020: MLS observations of chemical processes and comparisons with previous extreme winters

Gloria L Manney[1,1], Nathaniel J Livesey[2,2], Michelle L. Santee[2,2], Lucien Froidevaux[3,3], Alyn Lambert[4,4], Zachary Lawrence[5,5], Luis Millan[6,6], Jessica L. Neu[7,7], William G. Read[4,4], Michael J. Schwartz[8,8], and Ryan Fuller[9,9]

[1]Northwest Research Associates
[2]Jet Propulsion Laboratory
[3]JPL/California Institute of Technology, California, USA
[4]Jet Propulsion Lab (NASA)
[5]NOAA Physical Sciences Laboratory
[6]Jet propulsion laboratory
[7]Jet Propulsion Laboratory / Caltech
[8]Jet Propulsion Laboratory, California Institute of Technology
[9]Jet Propulsion Laboratory, California of Technology

November 30, 2022

Abstract

Aura Microwave Limb Sounder (MLS) measurements show that chemical processing was critical to the observed record-low Arctic stratospheric ozone in spring 2020. The 16-year MLS record indicates more denitrification and dehydration in 2019/2020 than in any Arctic winter except 2015/2016. Chlorine activation and ozone depletion began earlier than in any previously observed winter, with evidence of chemical ozone loss starting in November. Active chlorine then persisted as late into spring as it did in 2011. Empirical estimates suggest maximum chemical ozone losses near 2.8 ppmv by late March in both 2011 and 2020. However, peak chlorine activation, and thus peak ozone loss, occurred at lower altitudes in 2020 than in 2011, leading to the lowest Arctic ozone values ever observed at potential temperature levels from ~400–480 K, with similar ozone values to those in 2011 at higher levels.

Record-low Arctic stratospheric ozone in 2020: MLS observations of chemical processes and comparisons with previous extreme winters

Gloria L Manney[1,2], Nathaniel J Livesey[3], Michelle L Santee[3], Lucien Froidevaux[3], Alyn Lambert[3], Zachary D Lawrence[4,1], Luis F Millán[3], Jessica L Neu[3], William G Read[3], Michael J Schwartz[3], Ryan A Fuller[3]

[1]NorthWest Research Associates, Socorro, NM, USA
[2]New Mexico Institute of Mining and technology, Socorro, NM, USA
[3]Jet Propulsion Laboratory, California Institute of Technology, Pasadena, CA, USA
[4]National Oceanic and Atmospheric Administration / Cooperative Institute for Research in Environmental Sciences, Boulder, CO, USA

Key Points:

- MLS trace gas data show that exceptional polar vortex conditions led to record-low ozone in the Arctic lower stratosphere in 2019/2020
- Early and persistent cold conditions led to the longest period with chlorine in ozone-destroying forms in the 16-year MLS data record
- Chemical ozone destruction began earlier than in any Arctic winter in the MLS record and ended later than in any year except 2010/2011

Corresponding author: Gloria L Manney, `manney@nwra.com`

Abstract

Aura Microwave Limb Sounder (MLS) measurements show that chemical processing was critical to the observed record-low Arctic stratospheric ozone in spring 2020. The 16-year MLS record indicates more polar denitrification and dehydration in 2019/2020 than in any Arctic winter except 2015/2016. Chlorine activation and ozone depletion began earlier than in any previously observed winter, with evidence of chemical ozone loss starting in November. Active chlorine then persisted as late into spring as it did in 2011. Empirical estimates suggest maximum chemical ozone losses near 2.8 ppmv by late March in both 2011 and 2020. However, peak chlorine activation, and thus peak ozone loss, occurred at lower altitudes in 2020 than in 2011, leading to the lowest Arctic ozone values ever observed at potential temperature levels from ∼400–480 K, with similar ozone values to those in 2011 at higher levels.

Plain Language Summary

Unlike the Antarctic, the Arctic does not usually experience an ozone hole because temperatures are often too high for the chemistry that destroys ozone. In 2019/2020, satellite measurements show record-low stratospheric wintertime temperatures and record-low springtime ozone concentrations in the Arctic lower stratosphere (about 12–20 km altitude). Only one other winter/spring season, 2010/2011, in this 16-year satellite data record comes close. Low temperatures, which result in chlorine being converted from non-reactive forms into forms that destroy ozone, started earlier than in any previous Arctic winter in the record and lingered later than in any year except 2011. The ozone-destroying chemistry in 2019/2020 occurred at lower altitudes (where more of the ozone that filters out harmful ultraviolet radiation resides) than in 2010/2011. Such extensive ozone loss can have important health and biological impacts because it leads to more ultraviolet radiation reaching the Earths surface. While the success of the Montreal Protocol in limiting human emissions that increase ozone-destroying gases in the stratosphere has resulted in much less Arctic ozone destruction than we would have otherwise had, future temperature changes could lead to other winters with even more chemical ozone depletion than in 2019/2020.

1 Introduction

Arctic chemical ozone loss varies dramatically because of extreme interannual variations in the meteorology of the stratospheric polar vortex (e.g. WMO, 2018). For the past 16 years, the Aura Microwave Limb Sounder (MLS) has provided a uniquely comprehensive suite of daily global measurements for studying lower stratospheric polar chemical processing. The two previous Arctic winters on record with coldest conditions and greatest ozone loss occurred during this period: In 2010/2011, although lower stratospheric minimum temperatures did not consistently set records, exceptionally prolonged (lasting into April) cold led to unprecedented Arctic chemical ozone loss (e.g., Manney et al., 2011; Sinnhuber et al., 2011; Kuttippurath et al., 2012; WMO, 2014). December 2015–January 2016 Arctic temperatures were the lowest in at least 68 years (Manney & Lawrence, 2016; Matthias et al., 2016), Arctic denitrification and dehydration were the most severe in the MLS record (e.g., Manney & Lawrence, 2016; Khosrawi et al., 2017), and ozone dropped more rapidly than in 2010/2011. Cumulative ozone loss did not match or surpass that in 2011 only because a major final warming in early March 2016 halted chemical processing and dispersed processed air from the vortex (Manney & Lawrence, 2016; Johansson et al., 2019). In 2019/2020, lower stratospheric temperatures were persistently below the threshold for chemical processing earlier than in any other year observed by MLS and remained low approximately as late as in 2011 (Lawrence et al., 2020, describe stratospheric vortex meteorology in 2019/2020).

We use MLS version 4 data (Livesey et al., 2020, see supporting information, hereinafter "SI", for additional details) and meteorological fields from the Modern Era Retrospective Analysis for Research and Applications Version 2 (MERRA-2) (Gelaro et al., 2017) to show lower stratospheric polar processing in the extraordinary 2019/2020 winter/spring Arctic vortex, resulting record-low ozone, and comparisons with the previous Arctic winters (2010/2011 and 2015/2016) with largest ozone losses.

2 Results

Figures 1a–g show Northern Hemisphere (NH) MLS maps in December 2010, 2015, and 2019 at 520 K (∼18 km; approximate level with most polar processing at this time). N_2O within the polar vortex was substantially lower (and H_2O higher) by early December 2020 than in either 2015 or 2010, and its gradients across the vortex edge were steeper, consistent with a stronger signature of confined descent and/or descent of lower values from above. By 9 December, the region of temperatures below the nitric acid trihydrate (NAT) polar stratospheric cloud (PSC) threshold (Hanson & Mauersberger, 1988) was larger and more concentric with the vortex in 2019 and 2015 than in 2010. Temperatures remained consistently below this threshold starting earlier in 2019 (by mid-November) than in either 2010 (which did not become cold particularly early) or 2015 (which did) (Lawrence et al., 2020). HNO_3 was depressed in part of the vortex by 9 December in both 2019 and 2015, but only 2019 showed substantial chlorine activation; much of the sunlit portion of the vortex was filled with high ClO by 1 December 2019, with correspondingly low HCl values (note that the gridding can make high HCl and high ClO overlap slightly, see SI). Typically, lower stratospheric ozone (O_3) is higher near the vortex edge than in its core before the onset of chemical loss and increases through late December (as in 2015 and 2010). In 2019, however, O_3 was already lower throughout the vortex (even near the inside edge) than outside by 1 December and continued to decline through the month, while it continued increasing outside the vortex as in other years. Along with the early chlorine activation, this suggests very early onset of chemical O_3 loss.

Figures 1h–n show 460 K (∼16 km; approximate level with most ozone loss) maps on dates when extreme values were seen in the polar vortex. By 26 March 2020, N_2O throughout the vortex was even lower compared to other years (and H_2O in regions unaffected by ice PSCs higher) than in December, consistent with an unusually strong confined descent signature. In contrast, temperatures remained below the ice PSC threshold much longer in 2016 than in any other Arctic winter on record (Manney & Lawrence, 2016; Matthias et al., 2016), leading to unprecedented dehydration (Khosrawi et al., 2017). HCl was slightly lower in 2020 than in 2011, which had lower HCl than 2016; consistent with this, ClO was comparably high in 2020 and 2011, and somewhat lower in 2016. MLS recorded no data during 27 March–19 April 2011 because of an instrument anomaly (e.g. Manney et al., 2011). By 26 March, 460 K O_3 was distinctly lower in 2020 than in 2011 and remained so through late April, when values started to rise in both years as the vortex weakened. Maps of trace gas extrema on MLS retrieval levels (Figs. S1, S2) show consistent results, with lower minimum springtime O_3 values in 2020 than in 2011.

Figure 2 shows 460 K MLS trace gas evolution comparing 2019/2020 with 2015/2016 and 2010/2011 as a function of equivalent latitude (the latitude that would encompass the same area between it and the pole as each potential vorticity, PV, contour, Butchart & Remsberg, 1986) and time, providing a vortex-centered view. In 2019/2020, vortex temperatures (from MERRA-2, Fig. 2a) were comparable to those in 2010/2011 and much lower than climatology in late February through March. Late December through January 2015/2016 temperatures are still the lowest on record, with the longest period below the ice PSC threshold (e.g., Lawrence et al., 2020); however, since low temperatures are more common during these months than later on, the 2015/2016 temperatures were not as anomalous as those later in the season in 2020 and 2011. Temperatures were anomalously low much earlier in the 2019/2020 winter than in 2010/2011.

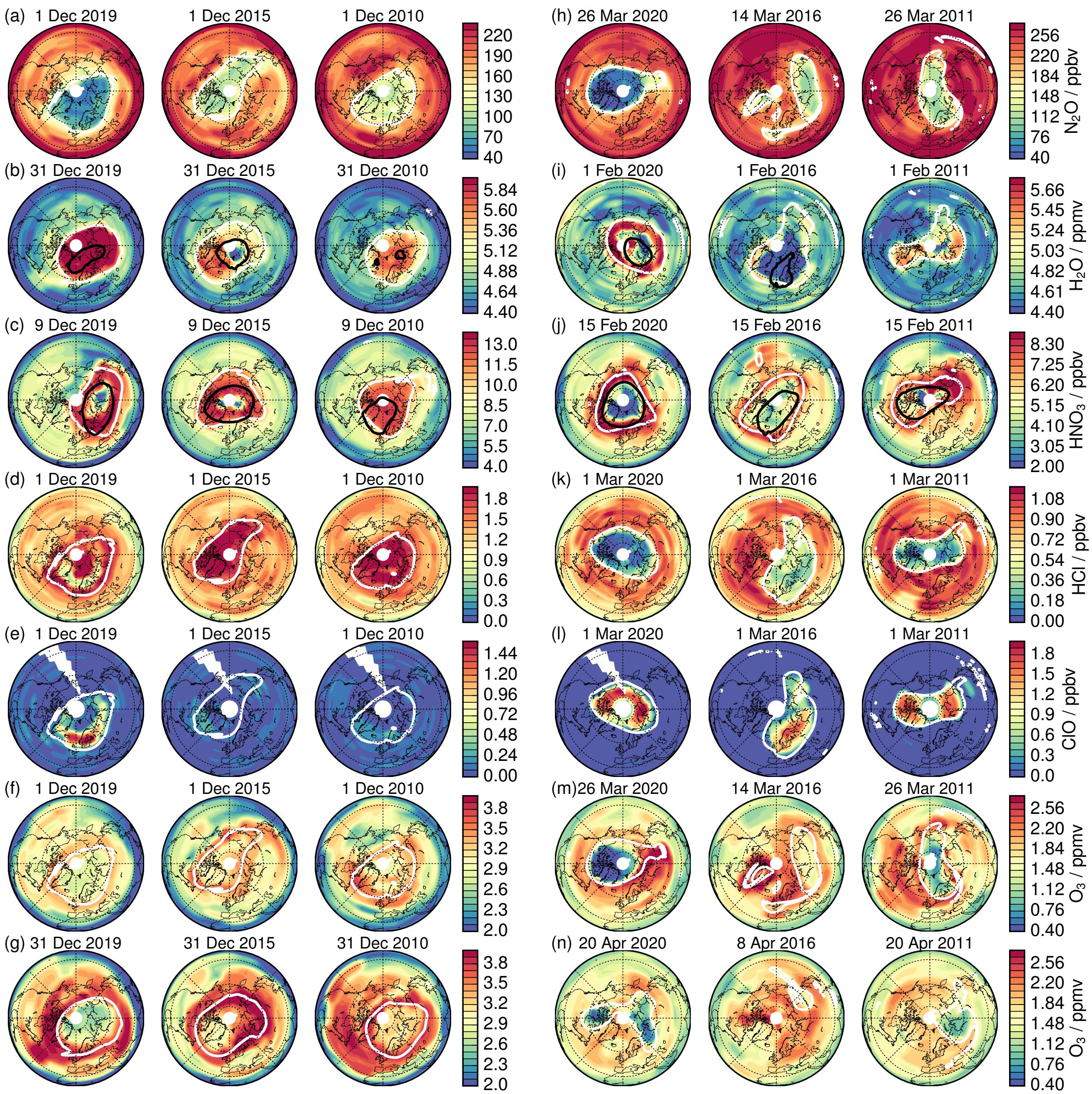

Figure 1. MLS maps: (a–g) 520 K in December and (h–n) 460 K on dates illustrating extreme values, for 2019/2020, 2015/2016, 2010/2011. Overlays: vortex boundary scaled potential vorticity (sPV, white; Lawrence et al., 2018; Lawrence & Manney, 2018); NAT (on HNO_3) and ice (on H_2O) PSC threshold temperatures (black; Lawrence et al., 2018). 26 March (20 April) (m–n for 2011, 2020) is the day before (day after) the 2011 data gap; earlier days are shown for O_3 in 2016 to capture its lowest values before vortex breakup.

Vortex strength (Fig. 2a, MERRA-2 overlays) particularly stands out in 2019/2020 (see also Lawrence et al., 2020), with PV gradient anomalies in late December 2019 comparable to those in mid-January 2011 and much stronger PV gradient anomalies as the season progresses than those in 2011 (the previous record-strong lower stratospheric vortex, e.g., Manney et al., 2011; Lawrence et al., 2020). The scaled PV (sPV) overlays in Figures 2b-g show that the 2019/2020 vortex also attained its maximum area earlier and maintained it longer than in other years; furthermore, the 2019/2020 vortex was larger than that in 2010/2011 throughout the winter.

Figures 2b,c show N_2O and H_2O as the difference from each year's 1 November field to emphasize changes in the confined descent signature through the winter. N_2O decreased more rapidly through February 2020 and developed steeper gradients across the vortex edge, clearly a stronger confined vortex descent signature than in previous years. Before temperatures reached ice PSC thresholds, H_2O also showed this signature, increasing faster in 2019/2020 than in other years. Work in progress indicates that this signature arises largely from a combination of descent of anomalously low N_2O/high H_2O entrained into the developing mid-stratospheric vortex and stronger vortex confinement in 2019/2020 than in the other years shown.

Consistent with the temperature and vortex evolution, gas-phase HNO_3 remained low longest in 2019/2020: Although negative HNO_3 anomalies were more pronounced in late December/January 2015/2016 and persisted later in 2011, in 2020 low anomalies appeared only slightly later than in 2016 and endured as late as in 2011. Moreover, since HNO_3 was anomalously high before the onset of PSCs in 2019/2020, the net decrease was similar to that in 2016. Significant denitrification occurred in both 2011 and 2016 (e.g., Manney et al., 2011; Khosrawi et al., 2017; Johansson et al., 2019), and similarly low HNO_3 values indicate extensive denitrification in 2020. Several multi-day periods with temperatures below the ice PSC threshold occurred in 2020, notably in late January, and a distinct signature of H_2O sequestration in PSCs is seen in early February; this drop (considering higher H_2O values before its onset) is comparable to the initial drop in 2016. Small negative or reduced positive anomalies near the vortex core persisted for about a month after temperatures rose above the ice PSC threshold in 2020, suggesting some dehydration; however, 2016 (when low anomalies lingered throughout the season) remains the only Arctic winter in which MLS observed vortex-wide dehydration.

Chlorine was activated through at least late January in most Arctic winters observed by MLS. HCl (Fig. 2e) dropped to anomalously low values as soon as the vortex was well-defined in 2019/2020 and 2015/2016, whereas chlorine activation in 2010/2011 was near average until late January. ClO values (Fig. 2f) before March depend strongly on vortex size and position since much of the vortex may be in darkness; nevertheless, anomalously high ClO during December 2019 (compared with near-climatological values until late December in the other years) highlights early chlorine activation in 2019/2020. ClO anomalies in March were similarly high in 2020 and 2011. Arctic chlorine deactivation normally proceeds though the reformation of $ClONO_2$ (e.g., Douglass et al., 1995). In all three years highlighted here, however, low-HNO_3, low-ozone, and low-temperature conditions shifted deactivation towards a more Antarctic-like pathway, with rapid HCl reformation (e.g., Douglass & Kawa, 1999). While we do not know the exact timing of deactivation in 2011 because of the instrument anomaly, the common periods MLS observed show similar patterns in 2020 and 2011.

The prolonged polar processing in 2019/2020 resulted in substantial low O_3 anomalies beginning in early January. Since we expect O_3 to increase via descent in the vortex, this pattern suggests appreciable chemical loss beginning by late November 2019. Strong low O_3 anomalies were apparent after early February 2016 and after early March 2011. The lowest O_3 observed in 2020 was much lower than that in 2011 at this altitude, and low values covered more area given the larger vortex. Although O_3 may have continued to decrease during the data gap in 2011, the area of very low O_3 was never comparable to that in 2020 (consistent with the extent of lowest values in Fig. 1 and lowest minimum values, Figs. S1 and S2).

Vortex averages of MLS data are provided in "Level 3" products that have recently been made public (Livesey et al., 2020, see SI for further description), and cross-sections of them (Fig. 3) show the vertical evolution of vortex trace gases. We focus on 2020 and 2011, since the extreme aspects of 2016 (discussed above) did not result in springtime O_3 loss comparable to that in 2020 or 2011. The N_2O and H_2O anomaly fields (and greater convergence in 2020 than in 2011 of the overlaid contours of N_2O values that were at 540 and 620 K on 1 November) show strong confined descent. Increased N_2O in April 2020 indicates the beginning of the vortex breakup at higher levels (Fig. 3a).

The area of potential PSC formation shifted farther downward over the winter in 2019/2020 (largest areas near 520–540 K in early winter and 460–480 K by spring) than in 2010/2011 (largest area near ∼520 K in early winter and ∼500 K by spring). Low HNO_3 anomalies follow this vertical progression. In 2019/2020, increasing high HNO_3 anomalies in late December and January below the cold region suggest renitrification through evaporation of PSCs sedimenting from above; similar, albeit smaller, anomalies were seen in January 2011. High H_2O anomalies during most of 2019/2020, consistent with the strong confined descent signature in N_2O, are related to initially low/high mid-stratospheric N_2O/H_2O; the abrupt shift from strong high anomalies to no significant anomalies in late January to early February 2020 reflects a period with substantial ice PSC activity. H_2O anomalies were weak in 2011 as ice PSCs were infrequent.

Chlorine activation as seen in HCl and ClO (Figs. 3d,e) is consistent with the evidence of PSC activity in temperatures and HNO_3: The region with greatest HCl depletion was at lower altitudes in winter/spring 2019/2020 than in 2010/2011 (spring minimum HCl values near ∼480 K in 2020 versus ∼520 K in 2011). Maximum ClO values were near 460 K throughout March 2020 and moved from ∼520 K to ∼480 K from early to late March in 2011. Anomalously high ClO in December 2019 and early January 2020 was consistent with HCl, but varied depending on how much of the vortex experienced sunlight; in contrast, HCl in December 2010 was slightly higher than climatology, indicating a relatively late start to chlorine activation.

Ozone contours (Fig. 3f) tilt downward through November, consistent with the strong descent signature seen in N_2O and H_2O. Since strong descent was ongoing through December, the flattening of O_3 contours and appearance of negative O_3 anomalies suggest that chemical O_3 loss began by late November and overwhelmed replenishment by descent by early December 2019. In 2011, strong negative O_3 anomalies first appeared in February. Although the 2011 MLS record is incomplete, no evidence suggests that O_3 reached values as low as those in 2020. Further, minimum vortex-averaged O_3 occurred near 440–460 K in 2020 but 480–500 K in 2011; thus even when values dipped as low in 2011, they were at smaller pressures and consequently affected the total column less. Record-low column ozone and associated record-high surface ultraviolet will be discussed in other papers in this special collection (e.g., Bernhard et al., 2020; Grooß & Müller, 2020; Wohltmann et al., 2020).

Vortex-averaged profiles on individual days (Fig. 3, right column) quantify differences between 2020 and 2011. Confined descent was stronger and PSC activity greater in 2020 than in 2011. Chlorine activation was similar at lower altitudes in both years but stronger at higher altitudes in 2011. O_3 abundances were smaller below ∼500 K in 2020 than in 2011. Fig. S3 shows raw MLS profiles indicating that, though vortex averages were only slightly lower in 2020 than in 2011, localized minimum values were near zero in late March 2020, compared to ∼0.5 ppmv in 2011, and occurred at lower altitude. Comparisons of time series of minima from ozonesondes and MLS data (Wohltmann et al., 2020) show consistent results.

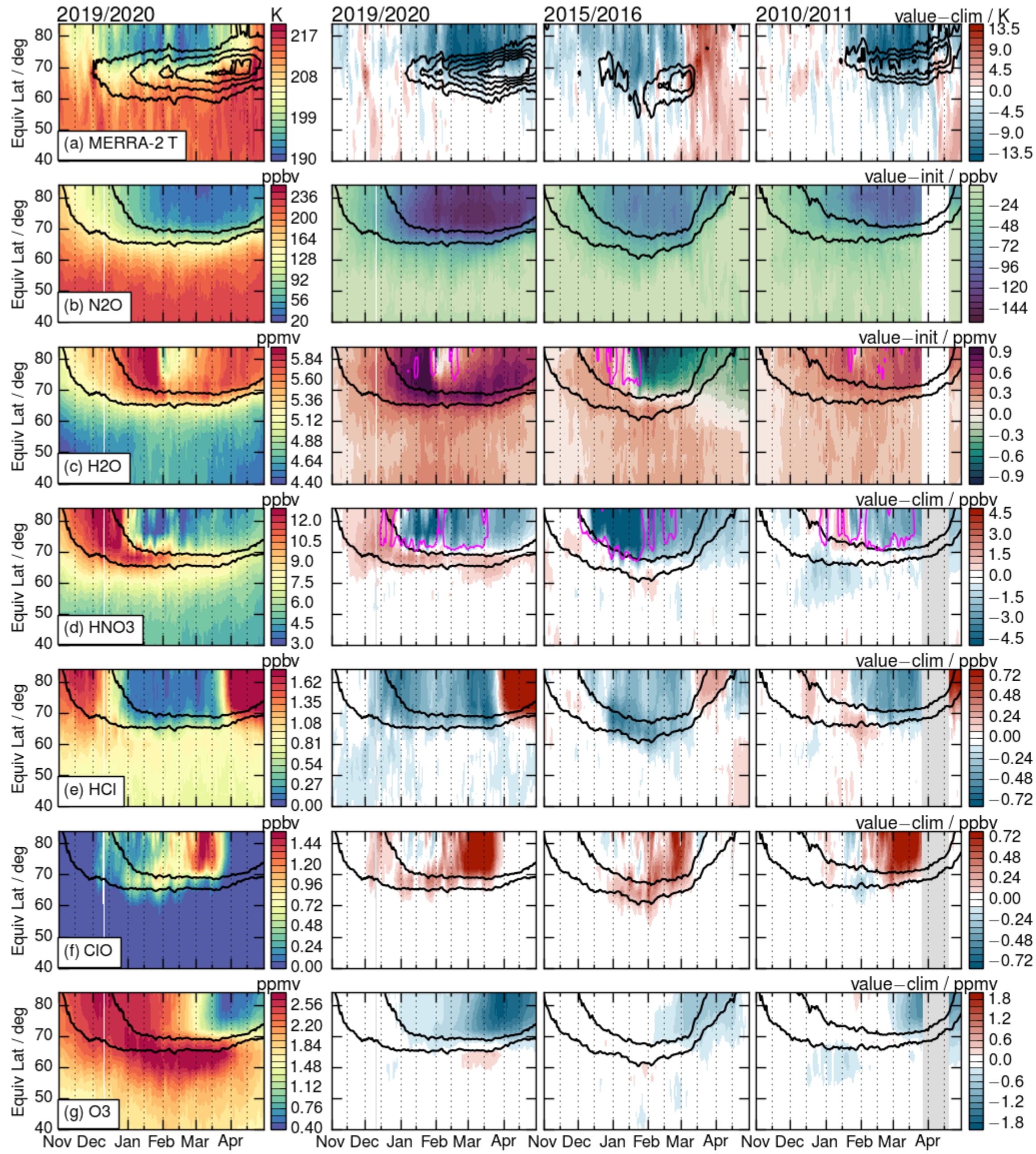

Figure 2. (a) 460 K EqL/time plots of MERRA-2 temperature for 2019/2020 (left), and difference from 2004/2005–2019/2020 climatology for (following columns) 2019/2020, 2015/2016, and 2010/2011; overlays: (left) sPV gradients with respect to EqL, and (remaining columns) sPV gradient differences from climatology (positive values only, showing where sPV gradients are stronger than climatology). (b–c) EqL/time plots of 460 K MLS N_2O and H_2O for 2019/2020 (left), and differences from the 1 November values (remaining columns). (d–g) As in (b–c), but for other MLS trace gases and differences from climatology; overlays: sPV in vortex edge region (black, 1.4, $1.8{\times}10^{-4}s^{-1}$), temperature (magenta; 197 K on HNO_3, 192 K on H_2O; values higher than the PSC thresholds, for NAT and ice, respectively, are shown to approximate the region where some values around the EqL contour are below those thresholds).

Figure 3g shows estimates of chemical O_3 loss using the "MLS Match" method (Livesey et al., 2015, also see SI). The computed cumulative chemical change in 2019/2020 indicates some early chemical loss above 520 K, but largest loss between about 400 and 470 K. Similar loss rates were computed for 2020 and 2011 through late March, with maximum losses near 2.8 ppmv. However, consistent with observed chlorine activation, maximum losses were at lower altitude in 2020 than in 2011.

3 Summary and Conclusions

Figure 4 summarizes chemical processing and ozone loss at 460 and 520 K in 2019/2020 in comparison to the other winters observed by Aura MLS. Descent of unusually low N_2O from the mid-stratosphere together with a well-isolated vortex resulted in smaller N_2O abundances in the lower stratosphere in 2020 than in any previous winter observed by MLS. Depressed gas-phase HNO_3 shows the onset of sequestration in PSCs in December; although the timing varied with altitude, the magnitude of the decrease was larger in 2019/2020. An abrupt drop in H_2O in late January 2020 indicates sequestration in ice PSCs, but temperatures rose above the ice PSC threshold again too soon to produce vortex-wide dehydration of similar magnitude to that in 2016. Although H_2O decreased over a small altitude range in 2020, at 460 K the drop during the coldest period was comparable to that in 2016 (and, when the altitude range is considered, larger than that in 2010 reported by, e.g., Khaykin et al., 2013).

Chlorine activation began slightly earlier in 2019 than in 2015 at 460 K and earlier than in 2010 at all levels. Previously, earliest strong Arctic chlorine activation was observed in 2012/2013, and the vortex was sufficiently exposed to sunlight for ClO to be elevated in late December (Manney et al., 2015). The timing of the HCl drop in 2019 was similar to that in 2012 at 460 K, but about ten days earlier at 520 K; at both levels highly elevated ClO was seen nearly two weeks earlier in 2019 than in 2012.

In 2011, chlorine deactivation occurred much later and followed a more Antarctic-like pattern than previously observed in the Arctic (e.g., Manney et al., 2011). The timing and pathway of chlorine deactivation in 2020 approximated Antarctic patterns even more closely. Not only did ClO remain enhanced at 460 K as late as in 2011, but also HCl recovered much faster than usual and reached considerably higher values by mid-April than in 2011. In a typical Arctic spring, deactivation initially proceeds through reformation of $ClONO_2$; however, several factors can shift Arctic chlorine partitioning toward HCl as in the Antarctic (e.g., Douglass et al., 1995; Santee et al., 2008). First, denitrification limits the availability of NO_2, inhibiting combination with ClO to form $ClONO_2$. In addition, low ozone and low temperatures together lead to preferential reformation of HCl (e.g., Douglass & Kawa, 1999). Thus HCl production was highly favored inside the persistently cold, strongly denitrified, and ozone-depleted Arctic vortex in spring 2020. Atmospheric Chemistry Experiment-Fourier Transform Spectrometer $ClONO_2$ data (Boone et al., 2013) (Fig. S6, Text S4) and model results (Grooß & Müller, 2020) are consistent with this picture.

These conditions resulted in record-low Arctic O_3 values in spring 2020 at levels below ∼500 K, and record low MLS stratospheric column values (see SI). Match estimates suggest more chemical loss in December 2019 through April 2020 than in 2010/2011 below ∼460 K; peak losses were near 2.8 ppmv in each of these winters, but at lower altitude in 2020 than in 2011. While empirical O_3 loss estimates have large uncertainties (e.,g., Griffin et al., 2019, also see SI), vortex-averaged descent calculations using MLS N_2O (overlaid lines/symbols in Fig. 4f,l) and using trajectory-based descent rates (overlaid symbols in Fig. 4) (see SI for description of calculations) give consistent results; Grooß and Müller (2020) and Wohltmann et al. (2020) report similar results using different datasets and methods. We find that chemical loss between December and March was very similar in the two winters, but significant chemical loss occurred in November only in 2019.

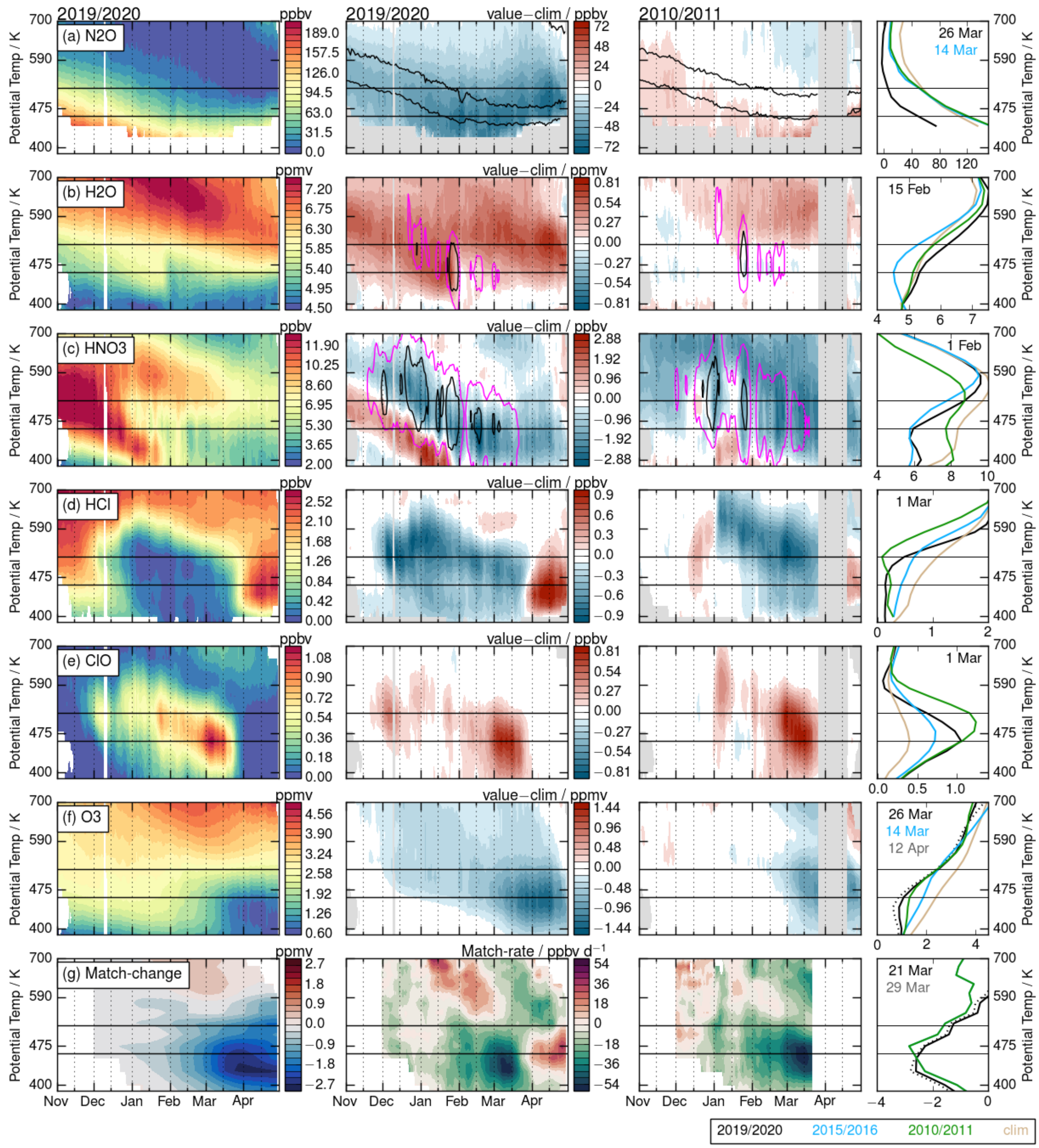

Figure 3. (a–f) Potential temperature/time sections of (left) 2019/2020 vortex-averaged (see SI) MLS species, and (center columns) differences from 2004/2005–2019/2020 climatology for 2019/2020 and 2010/2011; right column: 2011, 2016, and 2020 profiles on extreme dates, and climatology (for 2020 dates where those differ from other years). Black overlays in (a) show contours of N_2O values that were at 540 and 620 K on 1 November. Overlays in (b) show area with MERRA-2 temperatures below the ice PSC threshold (magenta shows 1% and black 2% of NH) and in (c) below the NAT threshold (magenta shows 3% and black 5% of NH). (g) (left) Cumulative chemical O_3 change in 2020 from Match (see text and SI), (center columns) Match rate of O_3 change in 2020 and 2011, and (right) cumulative O_3 change profiles on 21 March 2020 and 2011, and 29 March 2020 (dotted line). Horizontal lines mark 520 and 460 K. X-axis units for profiles are the same as left column of corresponding row.

(As explained in the SI, the vortex-averaged descent methods give slightly lower estimates than Match because they may be more affected by dilution of the chemical loss signature near the vortex edge.) Record-low springtime O_3 at lower altitudes in 2020 than in 2011 is consistent with evidence of record-low total column O_3 (Grooß & Müller, 2020; Wohltmann et al., 2020) and anomalously high surface ultraviolet in 2020 (Bernhard et al., 2020). Large interannual variability in meteorological conditions in the Arctic stratosphere (which led to the exceptionally strong and long-lived polar vortex in 2019/2020) may yet result in more extreme Arctic O_3 loss in future years while stratospheric chlorine loading remains high: For instance, 2015/2016 still stands out as the coldest Arctic winter with most denitrification and dehydration – if conditions such as those commenced as early in some future year and lasted as late as in 2019/2020, and the vortex remained well-isolated, then greater O_3 depletion could occur. This variability, coupled with likely effects of climate change, makes comprehensive monitoring of polar processes such as that provided by Aura MLS (currently in the 16th year of a 5-year mission) an important priority moving forward.

Acknowledgments

We thank the Microwave Limb Sounder team at JPL, especially Brian Knosp, for MLS retrieval processing, and computational, data processing, management, and analysis support; NASA's GMAO for providing their assimilated data products; and Germar Bernhard, Vitali Fioletov, Jen-Uwe Grooß, Rolf Müller, and Ingo Wohltmann for helpful discussions, and two anonymous reviewers for their careful and valuable comments. GLM and ZDL were partially supported by the JPL Microwave Limb Sounder team under JPL subcontracts to NWRA. Work at the Jet Propulsion Laboratory, California Institute of Technology was done under contract with the National Aeronautics and Space Administration. The datasets used here are publicly available:

- MERRA-2:
  https://disc.sci.gsfc.nasa.gov/uui/datasets?keywords=%22MERRA-2%22
- Aura MLS Level-2 and Level-3 data:
  https://disc.gsfc.nasa.gov/datasets?page=1&keywords=AURA%20MLS
- ACE-FTS v3.6 data: http://www.ace.uwaterloo.ca (registration required)

References

Bernhard, G. H., Fioletov, V. E., Grooß, J.-U., Ialongo, I., Johnsen, B., Lakkala, K., . . . Svenby, T. (2020). *Record-breaking increases in Arctic solar ultraviolet radiation caused by exceptionally large ozone depletion in 2020.* (to be submitted to GRL for this special collection)

Boone, C. D., Walker, K. A., & Bernath, P. F. (2013). Version 3 retrievals for the Atmospheric Chemistry Experiment Fourier Transform Spectrometer (ACE-FTS). In P. F. Bernath (Ed.), *The Atmospheric Chemistry Experiment ACE at 10: A solar occultation anthology* (pp. 103–127). A. Deepak Publishing.

Butchart, N., & Remsberg, E. E. (1986). The area of the stratospheric polar vortex as a diagnostic for tracer transport on an isentropic surface. *J. Atmos. Sci.*, *43*, 1319–1339.

Douglass, A. R., & Kawa, S. R. (1999). Contrast between 1992 and 1997 high-latitude spring Halogen Occultation Experiment observations of lower stratospheric HCl. *J. Geophys. Res.*, *104*(D15), 18,739–18,754.

Douglass, A. R., Schoeberl, M. R., Stolarski, R. S., Waters, J. W., III, J. M. R., Roche, A. E., & Massie, S. T. (1995). Interhemispheric differences in springtime production of HCl and $ClONO_2$ in the polar vortices. *J. Geophys. Res.*, *100*, 13,967–13,978.

Gelaro, R., McCarty, W., Surez, M. J., Todling, R., Molod, A., Takacs, L., . . .

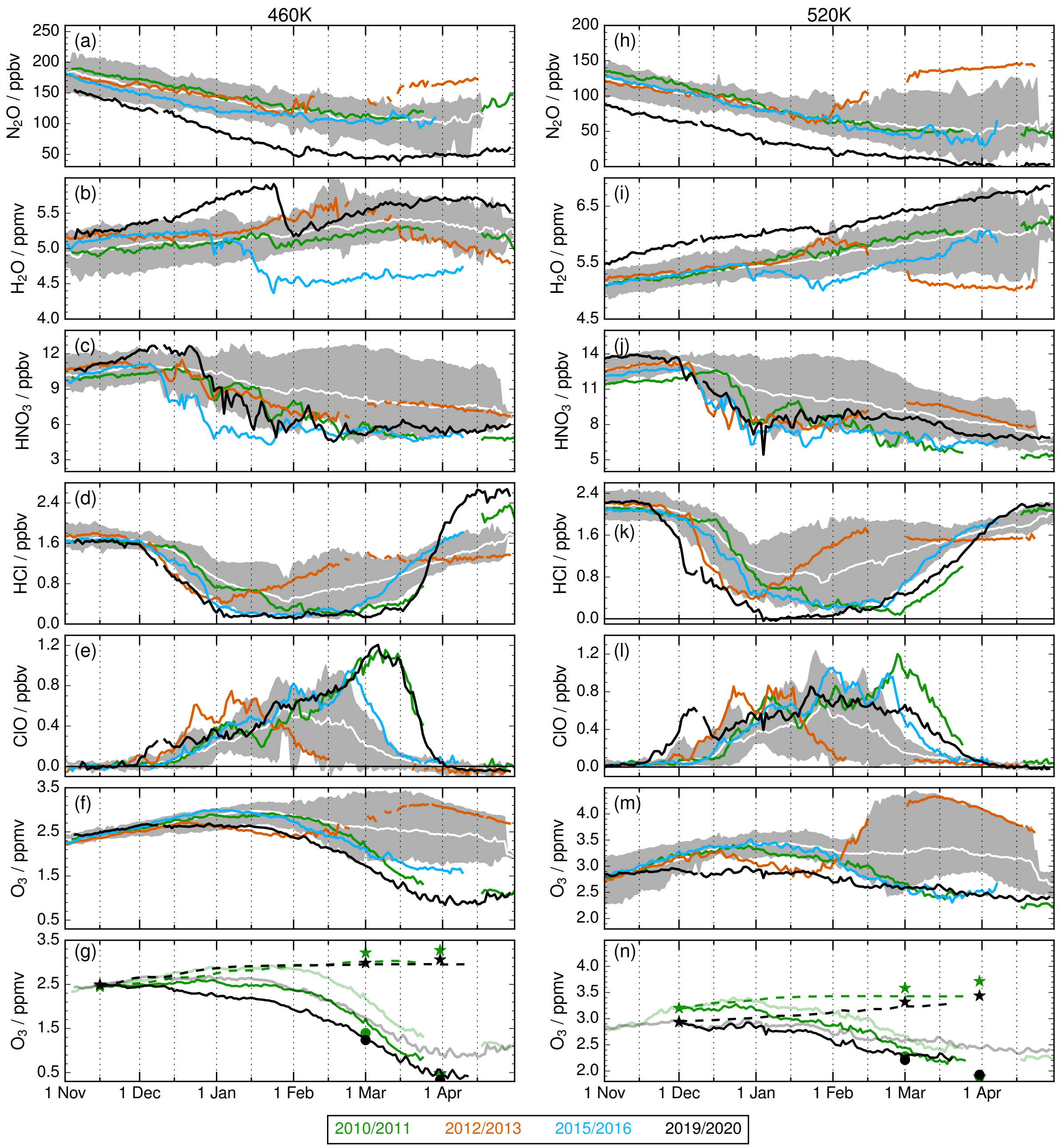

Figure 4. Vortex-averaged MLS trace gases for 2019/2020 (black), 2015/2016 (blue), 2012/2013 (orange), and 2010/2011 (green), at (a–g) 460 K and (h–n) 520 K. Grey envelope shows range of values for 2004/2005 through 2018/2019, excluding the highlighted years; white line shows mean for those years. (g) and (n) show passive ozone (dashed lines) and calculated chemical ozone loss (solid lines) estimated from MLS N_2O gradients (see SI) for 2011 (green) and 2020 (black), with observed evolution in pale colors; overlaid symbols show initial and passive ozone (stars) and trajectory-based chemical loss estimates (circles) (see SI); green triangles on 31 March (partially obscured by black circles) show 2011 chemical loss estimated using the average of two days bordering the data gap for the observed value.

Zhao, B. (2017). The Modern-Era Retrospective Analysis for Research and Applications, Version-2 (MERRA-2). *J. Clim.*, *30*, 5419–5454. doi: doi:10.1175/JCLI-D-16-0758.1

Griffin, D., Walker, K. A., Wohltmann, I., Dhomse, S. S., Rex, M., Chipperfield, M. P., … Tarasick, D. (2019). Stratospheric ozone loss in the Arctic winters between 2005 and 2013 derived with ACE-FTS measurements. *Atmos. Chem. Phys.*, *19*(1), 577–601. Retrieved from `https://www.atmos-chem-phys.net/19/577/2019/` doi: 10.5194/acp-19-577-2019

Grooß, J.-U., & Müller, R. (2020). *Simulation of the record Arctic stratospheric ozone depletion in 2020.* (Submitted to J. Geophys. Res.)

Hanson, D., & Mauersberger, K. (1988). Laboratory studies of the nitric acid trihydrate: Implications for the south polar stratosphere. *Geophys. Res. Lett.*, *15*, 855–858.

Johansson, S., Santee, M. L., Grooß, J.-U., Höpfner, M., Braun, M., Friedl-Vallon, F., … Woiwode, W. (2019). Unusual chlorine partitioning in the 2015/16 Arctic winter lowermost stratosphere: observations and simulations. *Atmos. Chem. Phys.*, *19*(12), 8311–8338. Retrieved from `https://www.atmos-chem-phys.net/19/8311/2019/` doi: 10.5194/acp-19-8311-2019

Khaykin, S. M., Engel, I., Vömel, H., Formanyuk, I. M., Kivi, R., Korshunov, L. I., … Peter, T. (2013). Arctic stratospheric dehydration. Part 1: Unprecedented observation of vertical redistribution of water. *Atmos. Chem. Phys.*, *13*, 11,503–11,517.

Khosrawi, F., Kirner, O., Sinnhuber, B.-M., Johansson, S., Höpfner, M., Santee, M. L., … Braesicke, P. (2017). Denitrification, dehydration and ozone loss during the 2015/2016 Arctic winter. *Atmos. Chem. Phys.*, *17*(21), 12893–12910. Retrieved from `https://www.atmos-chem-phys.net/17/12893/2017/` doi: 10.5194/acp-17-12893-2017

Kuttippurath, J., Godin-Beekmann, S., Lefèvre, F., Nikulin, G., Santee, M. L., & Froidevaux, L. (2012). Record-breaking ozone loss in the Arctic winter 2010/2011: comparison with 1996/1997. *Atmos. Chem. Phys.*, *12*, 7073–7085.

Lawrence, Z. D., & Manney, G. L. (2018). Characterizing stratospheric polar vortex variability with computer vision techniques. *Journal of Geophysical Research: Atmospheres*, *123*(3), 1510–1535. Retrieved from `http://dx.doi.org/10.1002/2017JD027556` (2017JD027556) doi: 10.1002/2017JD027556

Lawrence, Z. D., Manney, G. L., & Wargan, K. (2018). Reanalysis intercomparisons of stratospheric polar processing diagnostics. *Atmos. Chem. Phys.*, *18*, 13547–13579. doi: 10.5194/acp-18-13547-2018

Lawrence, Z. D., et al. (2020). *The remarkably strong Arctic stratospheric polar vortex of winter 2020: Ties to record-breaking Arctic oscillation and ozone loss.* (to be submitted to JGR for this special collection)

Livesey, N. J., Read, W. G., Wagner, P. A., Froidevaux, L., Lambert, A., Manney, G. L., … Lay, R. R. (2020). *EOS MLS version 4.2x level 2 and 3 data quality and description document* (Tech. Rep.). JPL. (Available from http://mls.jpl.nasa.gov/)

Livesey, N. J., Santee, M. L., & Manney, G. L. (2015). A Match-based approach to the estimation of polar stratospheric ozone loss using Aura Microwave Limb Sounder observations,. *Atmos. Chem. Phys.*, *15*, 9945–9963.

Manney, G. L., & Lawrence, Z. D. (2016). The major stratospheric final warming in 2016: dispersal of vortex air and termination of Arctic chemical ozone loss. *Atmos. Chem. Phys.*, *16*(23), 15371–15396. Retrieved from `https://www.atmos-chem-phys.net/16/15371/2016/` doi: 10.5194/acp-16-15371-2016

Manney, G. L., Lawrence, Z. D., Santee, M. L., Livesey, N. J., Lambert, A., & Pitts, M. C. (2015). Polar processing in a split vortex: Arctic ozone loss in early winter 2012/2013. *Atmos. Chem. Phys.*, *15*, 4973–5029.

Manney, G. L., Santee, M. L., Rex, M., Livesey, N. J., Pitts, M. C., Veefkind, P., …

Zinoviev, N. S. (2011). Unprecedented Arctic ozone loss in 2011. *Nature*, *478*, 469–475.
Matthias, V., Drnbrack, A., & Stober, G. (2016). The extraordinarily strong and cold polar vortex in the early northern winter 2015/2016. *Geophys. Res. Lett.*, *43*(23), 12,287–12,294. Retrieved from http://dx.doi.org/10.1002/2016GL071676 (2016GL071676) doi: 10.1002/2016GL071676
Santee, M. L., MacKenzie, I. A., Manney, G. L., Chipperfield, M. P., Bernath, P. F., Walker, K. A., ... Waters, J. W. (2008). A study of stratospheric chlorine partitioning based on new satellite measurements and modeling. *J. Geophys. Res.*, *113*. doi: 10.1029/2007JD009057
Sinnhuber, B.-M., Stiller, G., Ruhnke, R., von Clarmann, T., Kellmann, S., & Aschmann, J. (2011). Arctic winter 2010/2011 at the brink of an ozone hole. *Geophys. Res. Lett.*. doi: 10.1029/2011GL049784
WMO. (2014). *Scientific assessment of ozone depletion: 2014.* Geneva, Switzerland: Global Ozone Res. and Monit. Proj. Rep. 55.
WMO. (2018). *Scientific assessment of ozone depletion: 2018.* Geneva, Switzerland: Global Ozone Res. and Monit. Proj. Rep. 55.
Wohltmann, I., von der Gathen, P., Lehmann, R., Maturilli, M., Deckelmann, H., Manney, G. L., ... Rex, M. (2020). *Near complete local reduction of Arctic stratospheric ozone by severe chemical loss in spring 2020.* (Submitted to Geophys. Res. Lett.)

Supporting Information for "Record-low Arctic stratospheric ozone in 2020: MLS observations of chemical processes and comparisons with previous extreme winters"

Gloria L Manney[1,2], Nathaniel J Livesey[3], Michelle L Santee[3], Lucien Froidevaux[3], Alyn Lambert[3], Zachary D Lawrence[4,1], Luis F Millán[3], Jessica L Neu[3], William G Read[3], Michael J Schwartz[3], Ryan A Fuller[3]

[1]NorthWest Research Associates, Socorro, NM, USA

[2]New Mexico Institute of Mining and technology, Socorro, NM, USA

[3]Jet Propulsion Laboratory, California Institute of Technology, Pasadena, CA, USA

[4]National Oceanic and Atmospheric Administration / Cooperative Institute for Research in Environmental Sciences, Boulder, CO, USA

Contents of this file

1. Text S1 to S3
2. Figures S1 to S5

Introduction

The supplementary text provides further details of the Aura Microwave Limb Sounder (MLS) "Level 3" datasets and access (Text S1), brief descriptions of the "raw" MLS maps and profiles shown in Figs. S1 through S3 (Text S2), and details of the methods for empirical ozone loss estimates summarized in the main text (Text S3). The supplementary figures show maps of MLS extreme trace gas values taken directly from MLS Level 2 Geophysical Product (L2GP) data (Figs. S1 and S2) (related to Fig. 1 in the main text), minimum O_3 profiles taken directly from MLS L2GP data (Fig. S3) (related to Fig. 3 in the main text), and illustrations of details of "Match" empirical ozone loss estimates (Figs. S4 and S5) (described in Text S3, and related to Fig. 3 in the main text).

Text S1. MLS Level 3 Dataset and Details

The data used to make the maps shown in Fig. 1 in the main text are MLS "Level 2" (L2) data, which are daily data along the orbit tracks and on retrieval pressure levels. The Aura MLS science team has recently made public a "Level 3" (L3) dataset, described in more detail in Livesey et al. (2020). These products include daily and monthly binned values in several views, including "zonal" means in both geodetic (on retrieval pressure levels and potential temperature surfaces) and equivalent (on potential temperature surfaces) latitude, and the vortex averages used herein. These L3 products are now available as part of the MLS datasets from the NASA Goddard Space Flight Center Earth Science Data and Information Services Center (GES-DISC), at https://disc.gsfc.nasa.gov/datasets?page=1&keywords=AURA%20MLS. For the vortex averages in the L3 products, the vortex edge is defined using the altitude-dependent scaled potential vorticity (sPV) profile shown by Lawrence, Manney, and Wargan (2018), which was determined from a climatological average over the extended cold season of sPV values at the equivalent latitude of the maximum PV gradients. Lawrence and Manney (2018) discuss considerations related to different choices of vortex edge definition and show that this choice is robust over the season, including in the fall and spring when many other methods have difficulties.

The equivalent latitude / time series shown in Fig. 2 in the main text are from an internal L3 product produced by the MLS team that is similar to the publicly available L3 products but that has the bin averages weighted by "distance" in time and equivalent latitude from the bin centers and by the MLS L2 precision information. These products have previously been used and are described in numerous studies (e.g., Manney et al., 2015, and references therein).

Text S2. MLS Extreme Values from Level 2 Maps and Profiles Description

Figures S1 and S2show maps at 68 and 46 hPa of extreme values (maxima for ClO, minima for the other species) in MLS data obtained from the L2 profiles on retrieval pressure levels during January through early April in 2020, 2016, and 2011, giving a view of the raw data represented in the snapshots on isentropic surfaces shown in Fig. 1 in the main text. The maps are on a $4^\circ \times 2^\circ$ longitude-latitude grid and are produced by first applying a 3-point median filter to the daily L2GP MLS along-track trace gas values and then finding the extreme values occurring within each mapped spatial bin over the day 1 to 114 time period. The median filter provides a reduction in the visible spatial speckle (i.e. pixel to pixel noise) in the extreme value maps, but the results are not critical to the application of this process. The 3-point along-track filter extends over a spatial distance of about 500 km and is comparable to the spatial mapping scale. Consistent with the isentropic maps shown in the main text, 2016 has the lowest H_2O values (near 3 ppmv at 46 hPa), lower HNO_3 values than in 2011, and those low values (near zero) over a larger area/time than in 2020. Similar maximum ClO (over 2 ppbv) and minimum HCl (near zero) abundances are seen in each year, but the extremes are more frequent in 2011 and 2020 than in 2016, and they cover a larger region in 2020 than in 2011. Minimum ozone values are clearly much lower in 2020 than in 2011 (near 0/0.2 ppmv in 2020 and 0.9/0.7 ppmv in 2011 at 68/46 hPa).

Figure S3 further defines these minimum ozone values, showing that the lowest minima observed in 2011 were near 0.5 ppmv, compared with less than 0.1 ppmv in 2020. Of course, the true minimum for 2011 might have occurred during the data gap, but the 2020 minimum values on dates before and after the data gap in 2011 are also on the order of 0.5 ppmv lower than those in 2011. The lower stratospheric ozone decrease in this time period is not very different between 2020 and 2011. Because the 1 February minimum values were lower in 2020 than in 2011 (because of early onset of chemical loss, see main text), the profiles shown here suggest a similar rate of chemical ozone loss in February and March in the two years, consistent with the Match estimates shown below and in the main text.

The minimum ozone values shown here are consistent with results from a comparison of ozonesonde and MLS minimum ozone values for 2020, 2016, and 2011 (Ingo Wohltmann, personal communication).

Text S3. Empirical Ozone Loss Estimates Description

Empirical ozone loss estimates for 2020 and 2011 are done using several previously documented methods. In Fig. 3 we showed summary results of the MLS Match method described by Livesey, Santee, and Manney (2015). A few small changes have been made relative to that work: MERRA-2 rather than earlier GEOS-5.1/GEOS-5.2 data are used to drive the trajectory calculations. The vortex edge is now (here and throughout this paper) defined using the values from the potential temperature dependent profile of sPV (from Lawrence et al., 2018) used elsewhere in the paper; however, for the Match calculations, we add $+0.2\times10^{-4}\mathrm{s}^{-1}$ at each level to those values to minimize the possible impact of mixing across the vortex edge on the calculations. A limit of 10% on the change in sPV values along each trajectory is used (rather than the 25% mainly used by Livesey et al., 2015). Livesey et al. (2015) describe sensitivity tests for the vortex edge and sPV change parameters – in general, their results show that both of these changes tend to select for parcels that are farther inside the vortex, and thus it is not surprising that they often lead to slightly larger estimates of ozone loss (because they are expected to be less affected by any errors related to mixing across the vortex edge). Figures S4 and S5 illustrate the steps in the Match method that lead to the chemical ozone loss estimates shown in the main text, and show the details of the results for 2019/2020 and 2010/2011. The vortex area indicates the averaging region and the area within which the matches are identified. Since the reactions that destroy ozone depend on sunlight, the ozone hourly rate of change is computed per sunlit hour based on all the matches; the daily rate of change and cumulative change are then integrated from the hourly rate. To help assess the uncertainty in transport, a similar procedure is done for N_2O (shown in Figs. S4 and S5, panels f and g), except the rate does not take into account sunlit time. In both cases shown here, above 450 K, the Match procedure erroneously reports a "loss" in mid-stratosphere N_2O, suggesting (as discussed by Livesey et al., 2015) that it either underestimates descent (which would tend to result in underestimating the amount of chemical ozone loss) or overestimates mixing-in of higher N_2O extra-vortex air (the impact of which on inferred ozone loss is less clear, since the morphology of ozone with respect to the vortex edge varies with altitude and time such that it is not obvious whether mixing into the vortex would always decrease or increase ozone). Livesey et al. (2015) found that MLS Match results tended to be at the low end of ozone loss estimates compared to studies using other methods and/or datasets. However, later study showed that Match-based ozone loss estimates (such as those in this paper) using MERRA-2 rather than GEOS-5.1/GEOS-5.2 analysis fields are more in line with estimates using other techniques.

Figs. S4g and S5h show very similar amounts of ozone loss in 2020 and 2011 up through late March, but, consistent with the observed ozone profiles, with the peak chemical loss at lower altitude in 2020 than in 2011. A slightly earlier onset of chemical loss in 2020 is indicated, but significant ozone loss is not apparent before January, unlike the estimates based on vortex averaged descent described below. The vortex in the middle and upper stratosphere began to erode in late March (Lawrence et al., 2020, also seen here in N_2O in Fig. 3 in the main text), and Fig. S4 shows that the "inner vortex" for the Match averages becomes undefined at the highest levels shown. While "chemical" ozone change appears to decrease (except at the lowest levels shown) in April 2020, N_2O changes indicate increasing errors in transport that would be consistent with this, suggesting (consistent with chlorine being deactivated by this time) that chemical ozone loss ceased by about the end of March.

"Vortex-average descent methods" use a vortex-averaged ozone profile from observations at the beginning and end of the calculation period and an estimate (which can be obtained by several means) of vortex-averaged diabatic descent rates to estimate the ozone amount if the initial observation-based ozone values descended in the vortex via passive transport; the difference between this and the ozone profile at the end of the calculation then gives an estimate of the chemical loss (e.g., Griffin et al., 2019, and references therein). We used two means to estimate the diabatic descent rates here: First, we calculated the temporal and vertical (with respect to potential temperature) gradients of vortex averaged MLS N_2O and used those to estimate the rate at which it descended. Second, we ran back trajectories (using MERRA-2 fields) for dense grids of parcels from a set of "final" dates and averaged the descent of the parcels that were inside the vortex on those final dates for each earlier day in the run. For these calculations, parcels were initialized on a dense ($0.5^\circ \times 0.5^\circ$) equal-area grid encompassing mid- to high-latitudes, and run back for 90–150 days; the potential temperature of the parcels inside the vortex is then averaged for each day of the runs, giving an estimate of the descent over the period. We used the trajectory code described by Livesey et al. (2015) and Manney and Lawrence (2016, and references therein). The approach using N_2O ends up being limited in the vertical levels and time periods where reasonable estimates can be made because over the course of the winter N_2O descends far enough that near-zero values occupy most of the stratosphere, and only the lowest part of the stratosphere (below 500 K by late March 2020, a slightly higher level in 2011) has N_2O gradients strong enough that they can be used to track descent. Because of the particularly low N_2O values that were descending to the lower stratosphere in 2019/2020 (see Figs. 3 and 4 in main text), these estimates are even more limited during that year than during 2011. On the other hand, the trajectory-based descent grows increasingly more uncertain as the earliest date (the end date of the trajectory runs) is farther back, thus making results for the longer calculations even more uncertain. Furthermore, results from both methods are less certain when the vortex is less strong / well-confined, hence in November and April. Nevertheless, results from these two approaches for vortex averaged descent are generally consistent for the times / levels where both can be and were calculated. These estimates are slightly lower than those from the Match method because they are done using vortex averages over the full, rather than the inner, vortex region, and so include regions near the edge where the chemical loss signature may be diluted by mixing.

While we get fairly consistent results from each of the empirical ozone loss estimates we have made, particularly for the December through March period when the bulk of the chemical ozone loss takes place, it should be noted that there are large uncertainties in all methods of estimating ozone loss from observations (as discussed in some detail by Livesey et al., 2015; Griffin et al., 2019, and references therein). Comparison with results using other methods and datasets (to appear in this special collection) will be invaluable.

References

Griffin, D., Walker, K. A., Wohltmann, I., Dhomse, S. S., Rex, M., Chipperfield, M. P., ... Tarasick, D. (2019). Stratospheric ozone loss in the Arctic winters between 2005 and 2013 derived with ACE-FTS measurements. *Atmos. Chem. Phys.*, *19*(1), 577–601. Retrieved from `https://www.atmos-chem-phys.net/19/577/2019/` doi: 10.5194/acp-19-577-2019

Lawrence, Z. D., & Manney, G. L. (2018). Characterizing stratospheric polar vortex variability with computer vision techniques. *Journal of Geophysical Research: Atmospheres*, *123*(3), 1510–1535. Retrieved from `http://dx.doi.org/10.1002/2017JD027556` (2017JD027556) doi: 10.1002/2017JD027556

Lawrence, Z. D., Manney, G. L., & Wargan, K. (2018). Reanalysis intercomparisons of stratospheric polar processing diagnostics. *Atmos. Chem. Phys.*, *18*, 13547–13579. doi: 10.5194/acp-18-13547-2018

Lawrence, Z. D., et al. (2020). *The remarkably strong Arctic stratospheric polar vortex of* *winter 2020: Ties to record-breaking Arctic oscillation and ozone loss.* (to be submitted to JGR for this special collection)

Livesey, N. J., Read, W. G., Wagner, P. A., Froidevaux, L., Lambert, A., Manney, G. L., ... Lay, R. R. (2020). *EOS MLS version 4.2x level 2 and 3 data quality and description document* (Tech. Rep.). JPL. (Available from http://mls.jpl.nasa.gov/)

Livesey, N. J., Santee, M. L., & Manney, G. L. (2015). A Match-based approach to the estimation of polar stratospheric ozone loss using Aura Microwave Limb Sounder observations,. *Atmos. Chem. Phys.*, *15*, 9945–9963.

Manney, G. L., & Lawrence, Z. D. (2016). The major stratospheric final warming in 2016: Dispersal of vortex air and termination of Arctic chemical ozone loss. *Atmos. Chem. Phys. Disc.*, *16*. Retrieved from http://www.atmos-chem-phys-discuss.net/acp-2016-633/ doi: 10.5194/acp-2016-633

Manney, G. L., Lawrence, Z. D., Santee, M. L., Livesey, N. J., Lambert, A., & Pitts, M. C. (2015). Polar processing in a split vortex: Arctic ozone loss in early winter 2012/2013. *Atmos. Chem. Phys.*, *15*, 4973–5029.

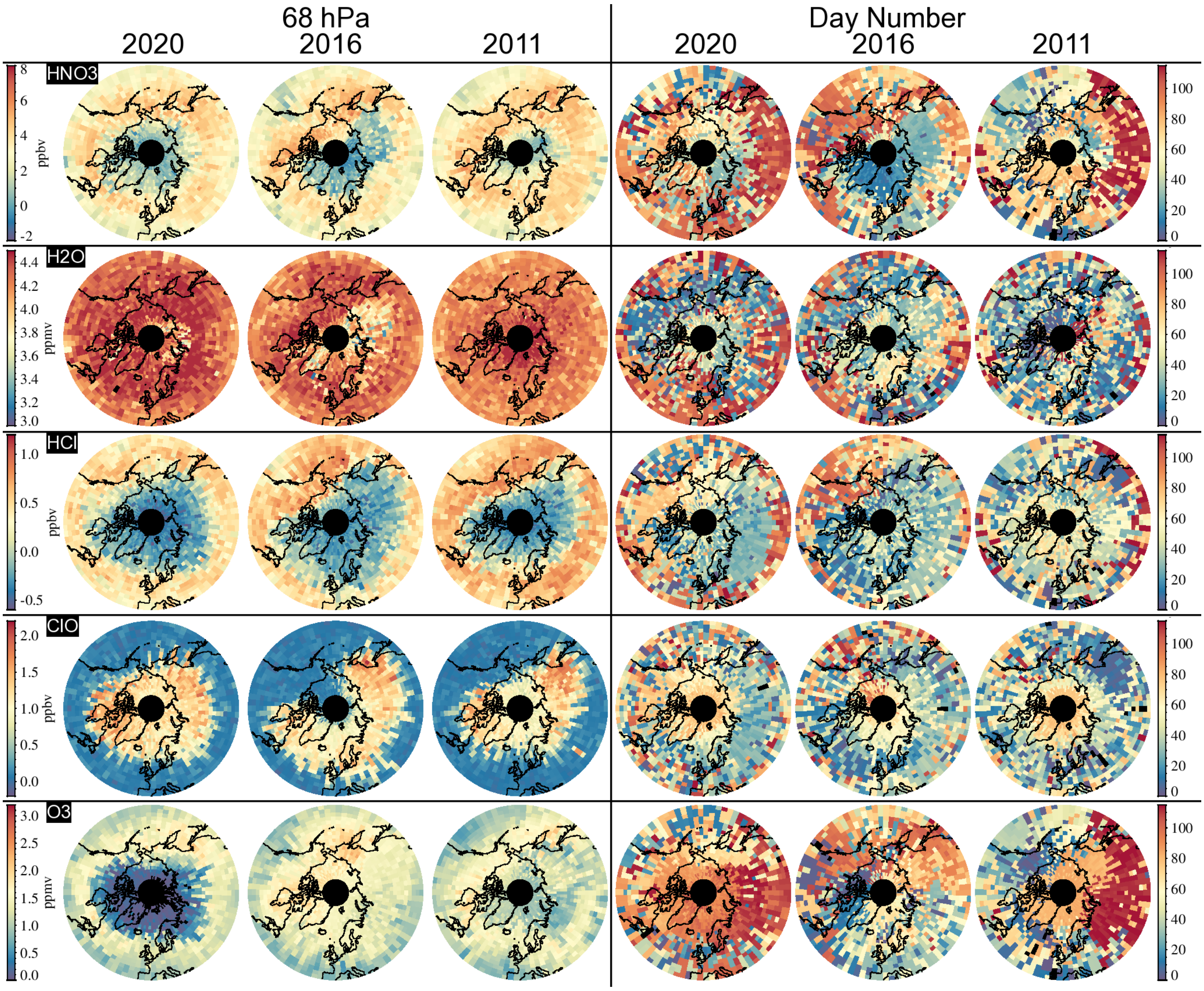

Figure S1. (Left columns) Maps of extreme MLS trace gas values for selected species at 68 hPa during January through early April in 2020, 2016, and 2011. Extrema are maxima for ClO and minima for all the other species shown. (Right columns) Corresponding maps of the day of occurrence (day number) of the extreme values.

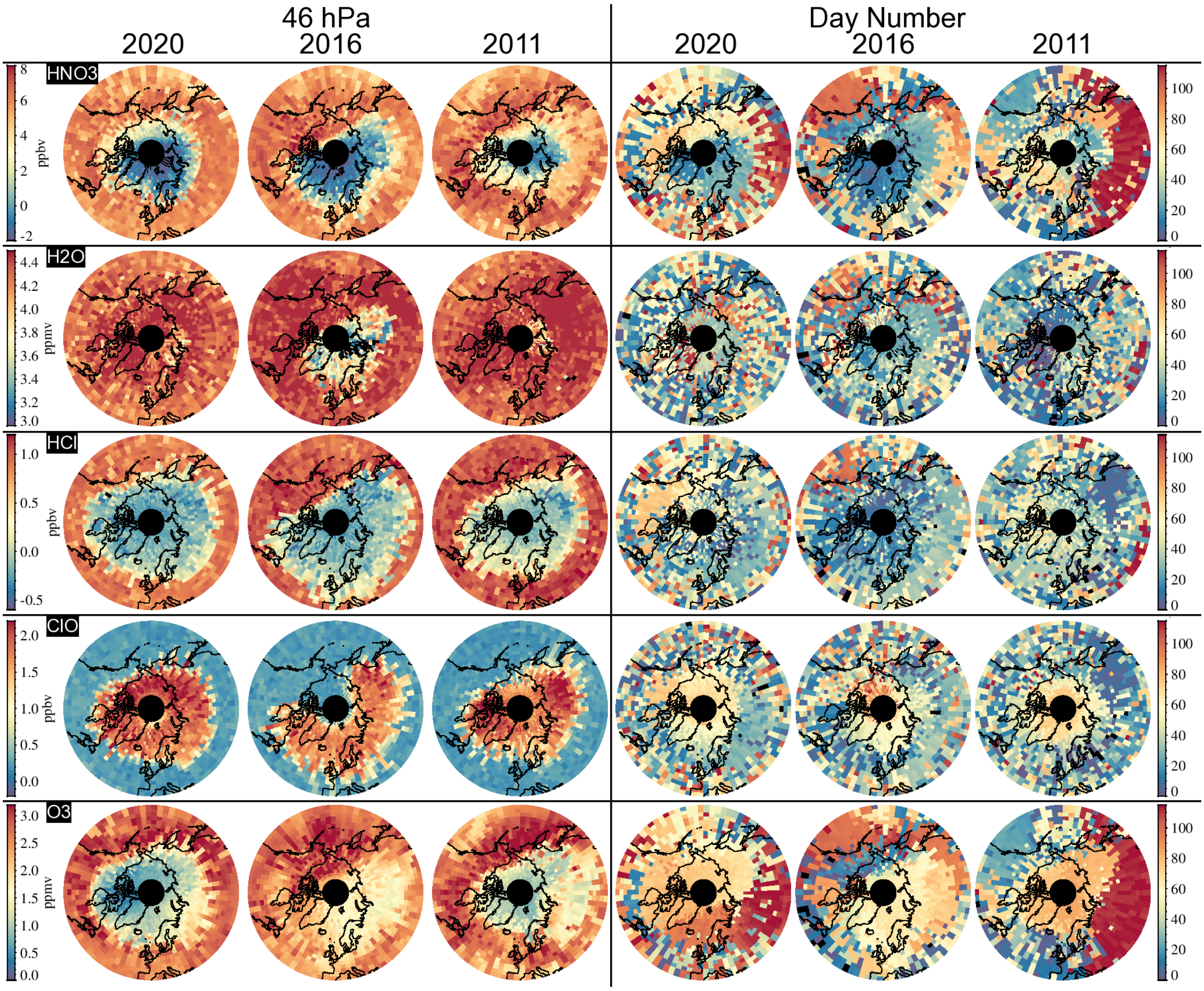

Figure S2. As in Fig. S1, but at 46 hPa.

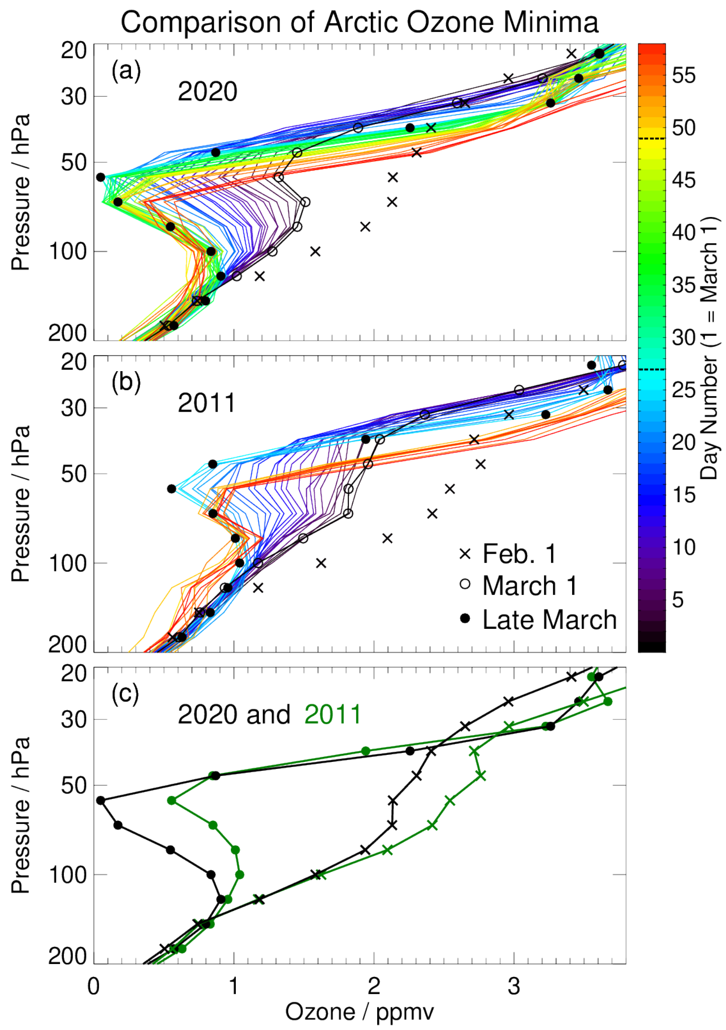

Figure S3. Minimum ozone mixing ratios for Arctic profiles in 2020 and 2011. Minima are obtained by considering the lowest 5% of the average mixing ratios between 82 and 46 hPa, covering the MLS ozone retrieval pressure levels with largest ozone decreases during February and March. (a) Minimum profiles for 2020, with 1 February (x-es), 1 March (open circles), and the lowest minimum in February/March (filled circles), in this case 27 March (day number 27 on the color bar). For clarity, we are not showing the minimum profiles before 1 March. (b) Same as (a) except for 2011; in this case, the minimum profile observed was on March 25; the color bar indicates (dashed horizontal lines) the range of days for which no MLS data were available (MLS was turned off from 27 March though 18 April). (c) Comparison of minima on 1 February (x-es) and in late March (filled circles) between 2020 (black) and 2011 (green).

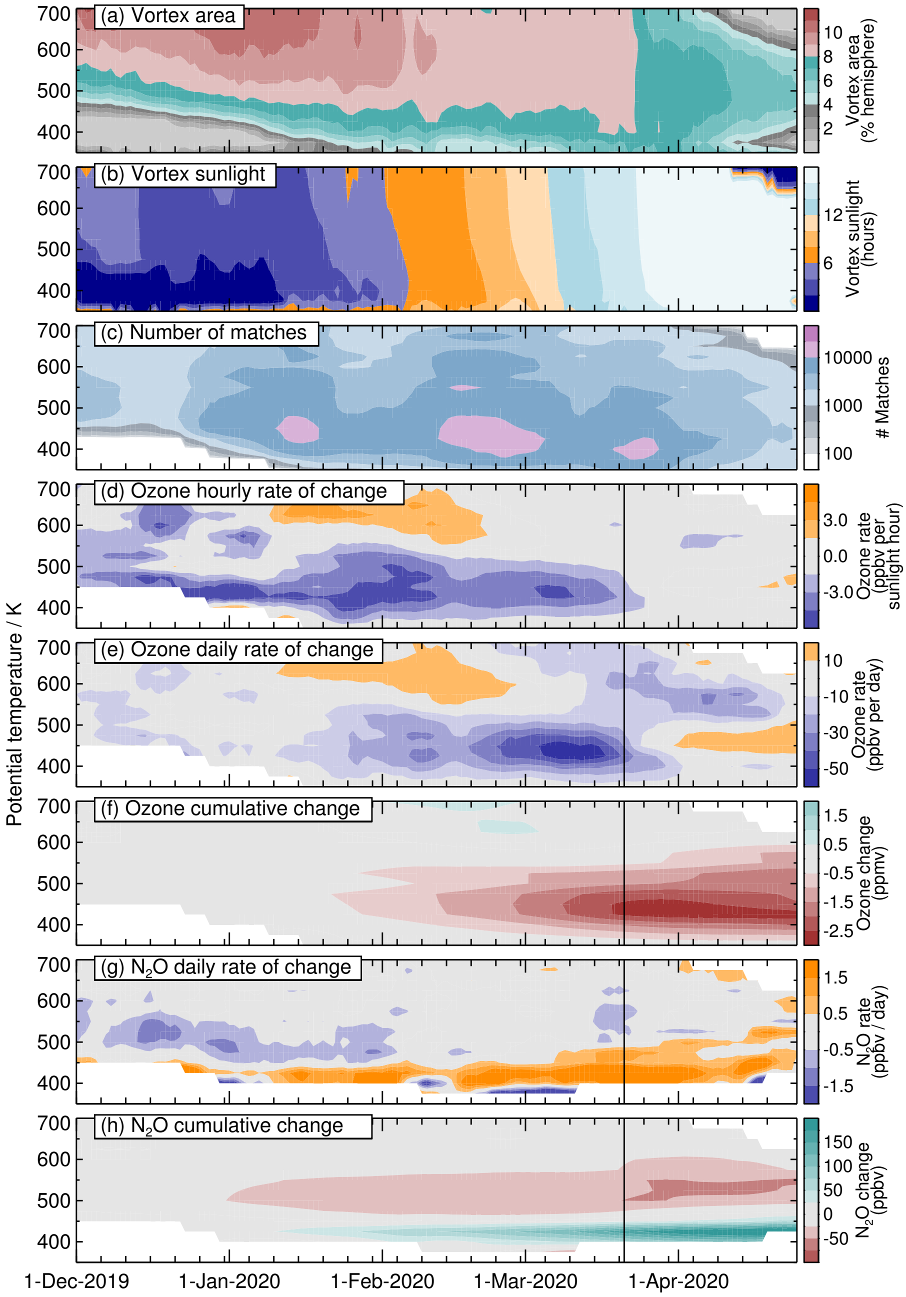

Figure S4. Temporal evolution of various height-resolved quantities during the 2019/2020 Arctic winter: (a) Polar vortex area (vortex edge defined per (Lawrence et al., 2018), with an offset of $+0.2\times10^{-4}$ s^{-1} as discussed above), expressed as a fraction of a hemisphere. (b) Average daily sunlight exposure time of air within the vortex. (c) Number of MLS matches in the vortex within a 15-day moving window in 25 K-thick potential temperature layers. (d) Estimated ozone loss rate per sunlight hour. (e) estimated daily ozone loss rate. (f) Cumulative ozone change. (g) N_2O daily rate of change. (h) N_2O cumulative change.

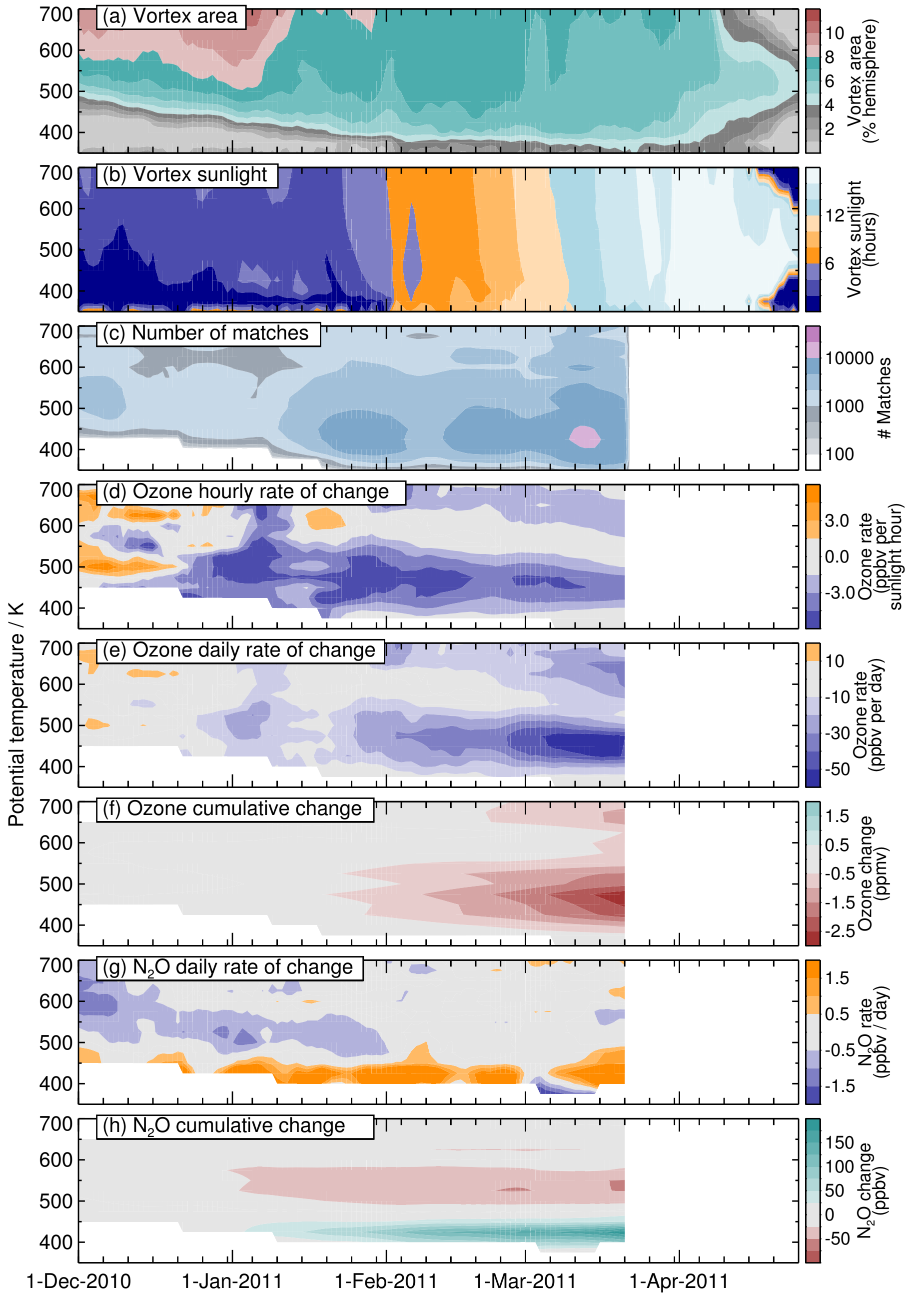

Figure S5. As Figure S4 but for the 2010/2011 Arctic winter/spring.